JOURNAL OF MATERIALS SCIENCE 28 (1993) 394–398

Solid state amorphization reactions in Ni/Ti multilayer composites prepared by cold rolling

T. D. SHEN, M. X. QUAN, J. T. WANG
State Key Laboratory of RSA, Institute of Metal Research, Academia Sinica, Wenhua Road 72, Shenyang 110015, Peoples' Republic of China

Solid state amorphizations in mechanically deformed Ni/Ti multilayer composites have been investigated by differential scanning calorimetry and X-ray diffraction. The growth of amorphous alloy in our Ni/Ti composites was facilitated by the large number of grain boundaries and relatively large degree of disorder induced in the metal layers by the cold rolling. The formation of different products of solid-state reaction in the Ni/Ti composites has been elucidated in terms of magnetic and enthalpy analysis. It is thought that the solid state amorphization occurs first during heating, followed by the formation of intermetallic compounds through direct solid-state reaction of elemental nickel and titanium and by the crystallization of the amorphous alloy already formed by the solid state amorphization reaction. The values of the activation energy for interdiffusion and interdiffusion coefficient for the formation of amorphous alloy in the Ni/Ti composites have also been calculated.

1. Introduction

Single-phase amorphous alloys can form in diffusion couples at relatively low temperatures by means of interdiffusion of pure, polycrystalline elements [1–7]. Amorphous material has been observed to grow to thickness of up to 100 nm at Ni/Zr interfaces [3, 4]. Therefore, it is possible by the solid-state amorphization reaction (SSAR) in multilayer composite to produce bulk amorphous alloys of basically any shape and size if one can prepare a very fine composite of the two crystalline components by mechanical deformation [8–11]. Although the equilibrium phase diagram and thermodynamic condition of the Ni/Ti and Ni/Zr systems are similar, it has been reported that the amorphous phase is not formed in the Ni/Ti system by isothermal annealing [12], while in a different investigation, the growth of amorphous alloy in Ni/Ti diffusion couples was observed only when a sufficient degree of disorder was initially present at the Ni/Ti interfaces [13]. Bulk amorphization in the Ni/Ti system has not been achieved so far, which was thought to be the result of too thick elemental layers, of an annealing treatment not yet optimized, or of thermodynamic conditions [11]. Therefore, many aspects of the SSAR are still unclear. In particular, the process of formation of the amorphous phase and the intermetallic compounds, and the roles of thermodynamic and kinetic parameters in the solid-state reaction of the Ni–Ti system need more discussion. In the present work we sought to investigate the SSAR in Ni/Ti multilayers prepared by cold rolling.

2. Experimental procedure

$Ni_{65}Ti_{35}$ (at %) composite powders (99.5%, 50–70 μm), in which a titanium core was coated by a thin layer of nickel, was used as a starting material. Ni/Ti multilayer was prepared by consolidating the composite powders, sealing it in a steel can and subsequently cold rolling the sample plus can. The samples obtained were then removed from the can and subsequently cold rolled in ten passes, each consisting of several (two to four) overlapping pieces of sample to increase its thickness, and rolling it to the thickness of the minimum spacing of the rollers (0.8 mm).

The average layer thickness in the multilayer composite was estimated from optical microscope (OM) and scanning electron microscope (SEM) observations on the cross-sections of the composite. The samples for observation of the polished surface were etched by a solution of HF (40%) 10 ml + H_2O 20 ml. The structure and phases of the samples were characterized by X-ray diffraction (XRD) and transmission electron microscopy (TEM). For the preparation of TEM samples, the sample was mixed with epoxy, and thin slices were cut along the direction of the surface of the sample with a hardened steel knife. The SSAR was also investigated by differential scanning calorimetry (DSC) and magnetic analysis. The saturation magnetization at room temperature was measured in a magnetic field up to 10 kOe.

3. Result and discussion

3.1. Process of cold rolling

Fig. 1 shows the cross-section morphology of the rolled samples. Compared with reported rolling techniques [14, 15], the deformation efficiency is rather high in our experiment when the Ni/Ti composite powders are utilized as a starting material. In fact, it is thought that Ni/Ti couples have been formed in the starting composite powders (CR0) with a single layer

0022–2461

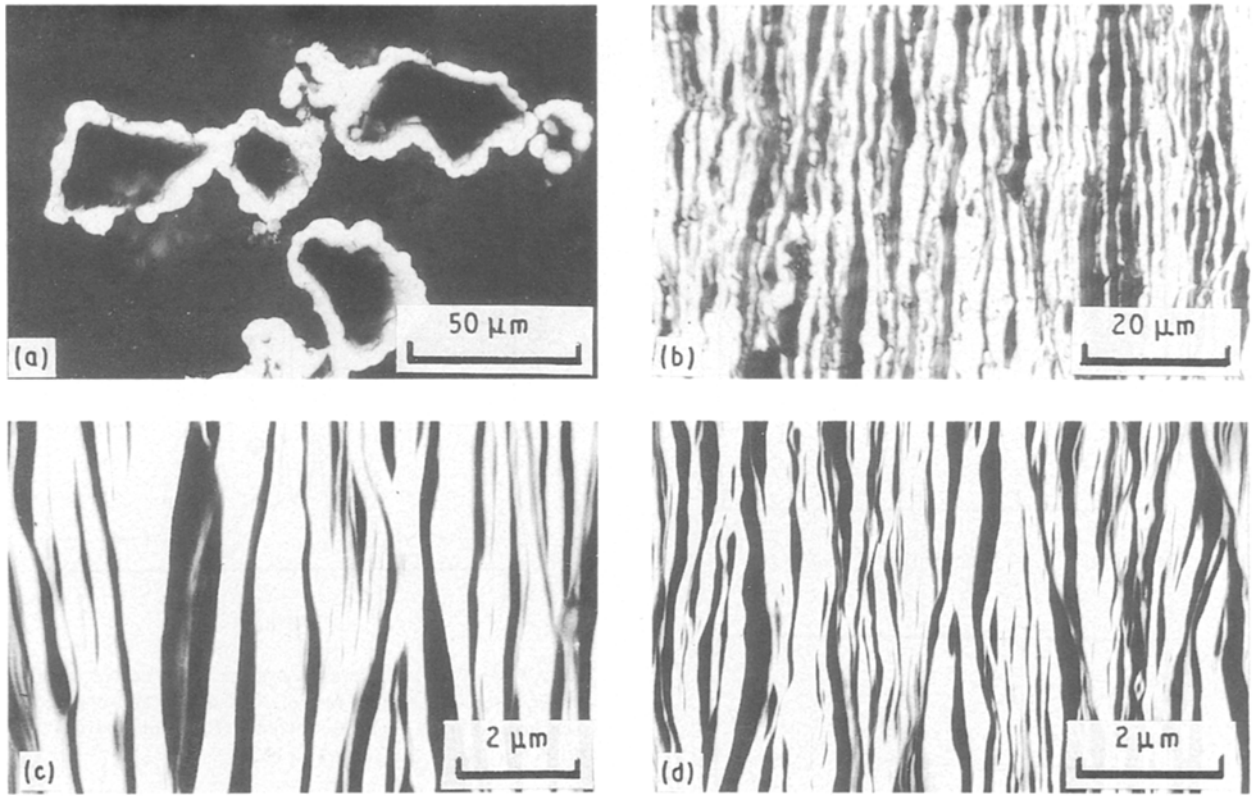

Figure 1 Cross-section morphology of the samples after (a) 0(CR0), (b) 2(CR2), (c) 8(CR8) and (d) 10(CR10) passes of rolling.

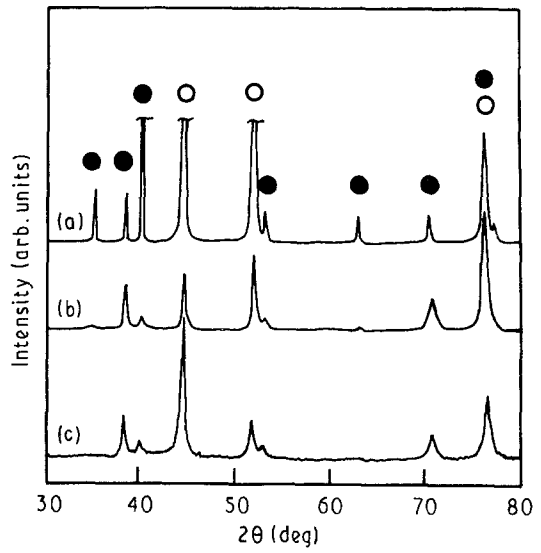

Figure 2 X-ray diffraction profiles of the samples after (a) 0(CR0), (b) 2(CR2) and (c) 10(CR10) passes of rolling. (○) Ni, (●) Ti.

thickness (SLT) of 5–35 μm. The SLT for Ni/Ti multilayer samples after 2(CR2), 8(CR8), 10(CR10) passes of cold rolling are about 1, 0.2 and 0.09 μm, respectively, as estimated from OM and SEM techniques.

Fig. 2 shows a sequence of X-ray diffractograms for $Ni_{65}Ti_{35}$. The initially sharp crystalline diffraction peaks are considerably broadened after several passes of rolling as a result of the refinement of the microcrystalline size and an internal strain. To separate these two effects, Williamson and Hall's approach [16] was used which utilizes the integral line width plotted against the scattering vector ($K = 4\pi \sin\theta/\lambda$). The crystallite size and lattice strain estimated by this approach in the CR10 sample are 29 nm and 0.35%, respectively. In comparison, the Scherrer formula, $D = 0.9\,\lambda/(\beta \cos\theta)$, provides a crystalline size of approximately 13 nm for titanium and 12 nm for nickel in the CR10 sample. A gradual formation of Ni–Ti amorphous alloy has been observed during mechanical alloying of the mixture of nickel and titanium powders, with a refinement of grain size and an increase of internal strain [17]. However, the amorphous phase has not been observed in the CR10 sample within the resolution of the X-ray diffraction technique.

3.2. Solid-state reaction in rolled samples

The DSC scans of different multilayer composites are shown in Fig. 3. There is no apparent reaction peak in the samples after four passes of rolling (CR4). At least two exothermic peaks are observed in CR8 and CR10 samples. For CR8 and CR10, the temperatures at which the heat release increases drastically as measured at a heating rate of 5 K min^{-1} (Fig. 3a), are 339 and 319 °C, respectively, indicating that the solid state reaction is easier to initiate with a decrease of single layer thickness. The exothermic peaks in CR10 are observed at various heating rates (Fig. 3b). The positions of the peaks shift to higher temperatures with an increase of the heating rate, indicating that the peaks are associated with heating-activated solid-state reactions.

X-ray diffraction profiles of CR10 samples heated to various temperatures at a heating rate of 30 K min^{-1} and consequently quenched are shown in Fig. 4. It can be conjectured from the profiles that the initial

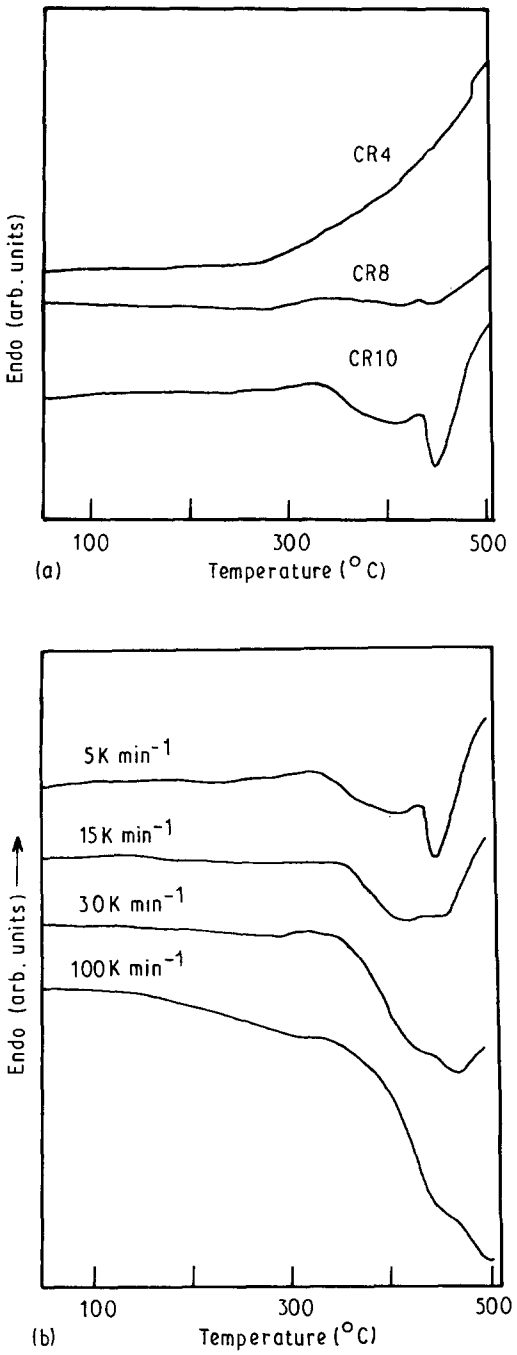

Figure 3 DSC scans of different composites. (a) CR4, CR8 and CR10 at a heating rate of 5 K min^{-1}, (b) CR10 at a heating rate of 5, 15, 30 and 100 K min^{-1}.

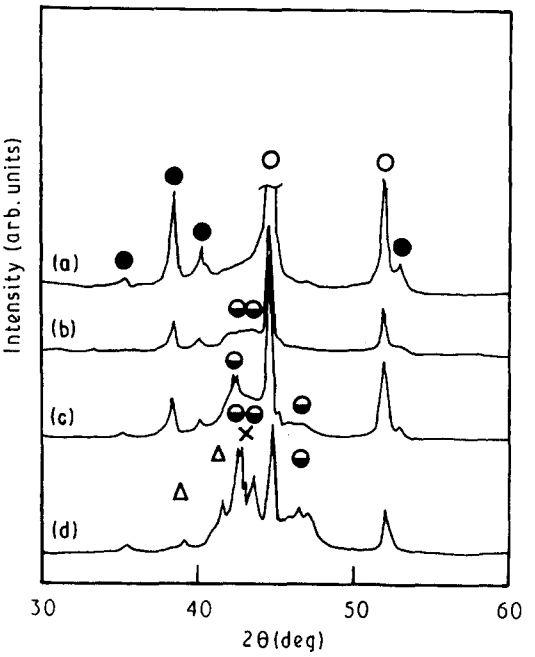

Figure 4 X-ray diffraction profiles of the CR10 heated to various temperatures at a heating rate of 30 K min^{-1} and consequently quenched. (a) 385 °C, (b) 400 °C. (c) 420 °C and (d) 500 °C. (○) Ni, (●) Ti, (◒) Ni_3Ti, (Δ) Ti_2Ni, (×) NiTi.

broad exothermic DSC signals observed in the lower temperature range (e.g. from 25–385 °C on the DSC scan at a heating rate of 30 K min^{-1}) is associated with the formation of an amorphous phase. The XRD profiles show Bragg peaks corresponding to elemental nickel and titanium, and a broad peak centered at $2\theta = 43.5°$ after the CR10 is heated to 385 °C (Fig. 4a). Such a broad Bragg peak is indicative of amorphous phase, and the angle of its maximum corresponds to that of liquid-quenched metallic glass of composition near $Ni_{63}Ti_{37}$ [18, 19]. Above 400 °C, XRD profiles reveal new Bragg peaks corresponding to intermetallic compounds Ni_3Ti, Ti_2Ni and NiTi, as shown in Fig. 4.

The microstructure and the corresponding selected-area diffraction pattern for the CR10 sample heated to 385 °C at a heating rate of 30 K min^{-1} are shown in Fig. 5. An amorphous area (Fig. 5a) is determined. The composition of the amorphous phase, as determined by EDAX, is $Ni_{64}Ti_{36}$, which is in good agreement with the XRD analysis. Fig. 5b shows an area of amorphous phase and nanocrystalline elemental nickel and/or titanium with an average crystalline size of 7 nm, the composition of the area is $Ni_{73}Ti_{27}$. This indicates that a large amount of nanocrystalline nickel and titanium, formed through severe mechanical deformation (99.5%), still exists in the samples even when heated to 385 °C. It can be considered that the nucleation of amorphous phase in the Ni/Ti interfaces is clearly facilitated by a relatively large degree of disorder induced by severe mechanical deformation. It should also be noted that a great number of grain boundaries produced by severe mechanical deformation may play an important role during the SSAR because the thermally propelled SSAR in a Ni/Ti multilayer occurs not only at the Ni/Ti interfaces but also along the grain boundaries, once the grain size of metal elements in the multilayer is as low as a few nanometres [20].

It has not been determined whether the Ni_3Ti, Ti_2Ni and NiTi come from crystallization of amorphous phases, or formed as a result of direct reaction of the elemental nickel and titanium in Ni/Ti multilayer composites prepared by mechanical alloying [21]. According to our analysis, part of the intermetallic compounds do come from the direct reaction of nickel and titanium. One piece of evidence is that the amount of elemental nickel and titanium in the CR10 samples heated to 500 °C is less than that in the CR10 to 385 °C, as shown in Fig. 4. In addition, the amount of heat release during the solid-state reactions can also give a reasonable explanation.

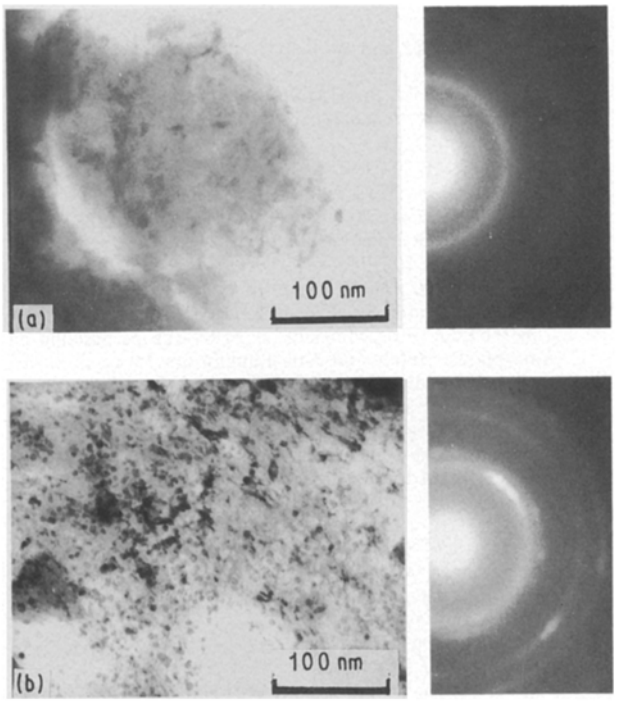

Figure 5 Transmission electron micrograph and a corresponding selected-area diffraction pattern of the CR10: (a) amorphous area, (b) amorphous and nanocrystalline area.

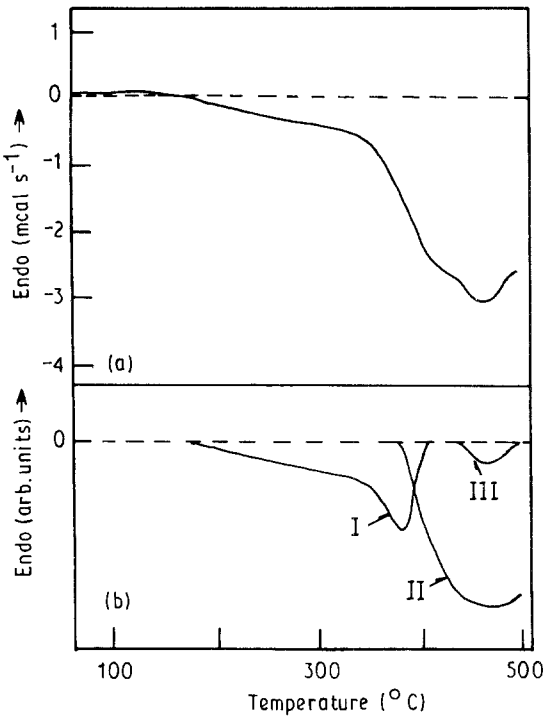

Figure 6 (a) DSC scan experimentally obtained at a heating rate of 30 K min^{-1} for the CR10 sample. (b) The corresponding schematic representation for solid-state reactions on the DSC scan: (I) low-temperature exothermic peak, (II) high-temperature large exothermic peak, and (III) high-temperature weak exothermic peak.

Elemental nickel is ferromagnetic, while elemental titanium and Ni–Ti amorphous alloy are not. Ignoring the change of atomic volume after mixing, the volume fraction of amorphous phase (X_{am}), in the CR10 sample after heating to 385 °C can be written as

$$X_{am} = (M_s^0 - M_s^1)(d_{Ti} + d_{Ni}X_{Ti}M_{Ti}/X_{Ni}M_{Ni})/[M_s^0(d_{Ti} - d_{Ni}) + M_s^{Ni}d_{Ni}] \quad (1)$$

where M_s^0, M_s^1 and M_s^{Ni} are the saturation magnetizations of starting CR0 sample, CR10 heated to 385 °C and pure elemental nickel, d_{Ti} and d_{Ni} are densities of titanium and nickel, X_{Ti} and X_{Ni} are atomic fractions of titanium and nickel in $Ni_{63}Ti_{37}$ amorphous alloy. M_{Ti} and M_{Ni} are the mole masses of titanium and nickel, respectively. According to Equation 1, X_{am} is 15.4% in the CR10 samples heated to 385 °C at a heating rate of 30 K min^{-1}. This volume fraction corresponds to an amorphous interlayer thickness of about 14 nm in a Ni/Ti bilayer. Therefore, bulk amorphization in the $Ni_{62}Ti_{38}$ composite has not been obtained [11]. The single layer thickness in the mechanically deformed $Ni_{62}Ti_{38}$ multilayer composite is 0.15 μm [11], which is even larger than that (0.09 μm) in our $Ni_{65}Ti_{35}$ multilayer composite.

X_{am} can also be obtained through analysis of heat release on the DSC scan. The formula can be written

$$X_{am} = \Delta H_T/\Delta H_{tot} \quad (2)$$

where ΔH_T is the area of the amorphization peak on a DSC scan integrated from the onset of the reaction to temperature T, ΔH_{tot} is the formation enthalpy of $Ni_{63}Ti_{37}$ amorphous alloy, which is about -31.4 KJ mol^{-1}, as calculated according to Miedema's model [22]. To measure the heat release on a DSC trace, the CR10 sample was heated at a rate of 30 K min^{-1} to 500 °C, followed by a second scan (identical thermal conditions) of the same sample; the data of the second scan were subtracted from the data of the first scan. The DSC scan obtained is shown in Fig. 6a. X_{am}, calculated according to Equation 2, is 15.3%, which is in good agreement with the results of magnetic analysis.

The heat, ΔH_x, of crystallization of the totally amorphous $Ni_{63}Ti_{37}$ alloy is about -3.0 KJ mol^{-1} [18]. If all the amorphous alloy formed in the CR10 sample heated to 385 °C crystallizes after the CR10 is heated to 500 °C, the total heat released during heating the CR10 sample from 25–500 °C can be calculated to be $15.4\% \times [-31.4 + (-3.0)] = -5.3$ KJ mol^{-1}. In fact, the total heat released measured by DSC is -21.9 kJ mol^{-1}. It is evident that the additional large heat release results from the direct reaction of elemental nickel and titanium into intermetallic compounds, this reaction has a heat release of -34.3 kJ mol^{-1} [23]. The volume fraction of intermetallic compounds, which exist in the CR10 heated to 500 °C through the direct reaction of nickel and titanium, as estimated from the additional heat release, is about 48%, while that through the crystallization of the amorphous alloy is not larger than 15.4%.

According to the above-mentioned, a schematic representation of solid-state reactions occurring during heating of the CR10 sample in the DSC may be shown as in Fig. 6b. The low-temperature exothermic peak (I) is associated with the formation of amorphous alloy through solid-state interdiffusion reaction, the high-temperature large exothermic peak (II) is associated with the formation of intermetallic compounds through direct solid-state reaction of elemental nickel

and titanium, and the high-temperature weak exothermic peak (III) is associated with the crystallization of the amorphous alloy.

3.3. Kinetic data for the SSAR

Using the DSC, kinetic data for the SSAR can be obtained through the analysis of the evolution of enthalpy [4]. It is believed that for at least part of the SSAR, the amorphous alloy grows by a diffusion-controlled layer process, and that the growing amorphous interlayer exhibits a linear concentration profile with constant interfacial compositions [24]. On this basis, a formula of DSC peak analysis for amorphous phase prepared by the SSAR can be written as

$$\ln(A(T)\mathrm{d}A(T)/\mathrm{d}t) = \ln\{f\tilde{D}_0(Sh)^2/[x(1-x)]\} - E/(kT) \quad (3)$$

where $A(T)$ is the area of the amorphization peak on a DSC trace integrated from the onset to temperature T, $\mathrm{d}A(T)/\mathrm{d}t$ is the heat flow in the DSC scan at temperature T, $\tilde{D}_0$ is the pre-exponential factor for interdiffusion coefficients, $\tilde{D}$, in amorphous $Ni_{63}Ti_{37}$, E is the activation energy for the formation of the amorphous phase, k is Boltzmann constant, f is the fractional concentration range over which the amorphous phase exists, S is the total interfacial area between nickel and titanium in the original CR10 sample, h is the enthalpy evolved per unit volume of amorphous phase formed, and x is the average composition of amorphous phase formed. For this Ni/Ti system, f, S, h and x are taken to be 0.44 [22], 8×10^{13} m^2, 3.9×10^8 J m^{-3} and 0.63, respectively. According to Equation 3, E, $\tilde{D}_0$ and $\tilde{D}$ (at 620 K) are calculated to be 1.34 eV atom^{-1}, 1.6×10^{-8} m^2 s^{-1} and 2.1×10^{-19} m^2 s^{-1}, which are of reasonable magnitudes compared with the published results, e.g. E was calculated to be 1.4 and 1.3 eV atom^{-1} in the compositionally modulated Ni/Ti multilayer films and electron-beam-deposited Ni/Ti bilayer thin films, respectively [25, 26], E and D_0 were calculated to be 1.2 eV atom^{-1} and 0.9×10^{-9} m^2 s^{-1} in the $Ni_{50}Ti_{50}$ multilayer composite powders mechanically alloyed for 15 h [21].

Acknowledgement

This work was supported by the National Natural Science Foundation of China.

References

1. R. B. SCHWARZ and W. L. JOHNSON, *Phys. Rev. Lett.* **51** (1983) 415.
2. W. L. JOHNSON, *Prog. Mater. Sci.* **30** (1986) 80.
3. E. J. COTTS, W. J. MENG and W. L. JOHNSON, *Phys. Rev. Lett.* **57** (1986) 2295.
4. R. J. HIGHMORE, J. E. EVETTS, A. L. GREER and R. E. SOMEKH, *Appl. Phys. Lett.* **50** (1987) 566.
5. K. SAMWER, *Phys. Rep.* **161** (1981) 1.
6. R. B. SCHWARZ and W. L. JOHNSON, *J. Less-Common Met.* **140** (1988) 1.
7. W. J. MENG, C. W. NIEH, E. MA, B. FULTZ and W. L. JOHNSON, *Mater. Sci. Engng* **97** (1988) 87.
8. L. SCHULTZ, Proceedings of the MRS Europe Meeting on "Amorphous Metals and Non-Equilibrium Process", Strasbourg 1984, edited by M. V. Allmen (Les Editions de Physique, Les Ulis, 1984) p. 135.
9. L. SCHULTZ, in "Proceedings of the 5th International Conference on Rapidly Quenched Metals", Wurzburg 1984, edited by S. Steeb and H. Warlimont (North-Holland, Amsterdam, 1985) p. 1585.
10. M. ATZMON, J. D. VERHOEVEN, E. D. GIBSON and W. L. JOHNSON, *ibid.* p. 1561.
11. L. SCHULTZ, "Amorphous and Liquid Materials". Proceedings NATO, Advanced, Study Institute Series (NASA, Passo della Mendola, 1985) p. 508.
12. W. J. MENG, B. FULTZ, E. MA and W. L. JOHNSON, *Appl. Phys. Lett.* **51** (1987) 661.
13. B. M. CLEMENS, *Phys. Rev. B* **33** (1986) 7615.
14. P. H. SHINGU, K. N. ISHIHARA, K. UENISHI, J. KUYAMA, B. HUNG and S. NASA, in "Solid State Powder Processing", edited by A. H. Clauer and J. J. de Barbadillo, (Minerals, Metals and Materials Society, Indianapolis, 1989) p. 21.
15. M. ATZMON, J. D. VERHOEVEN, E. D. GIBSON and W. L. JOHNSON, *Appl. Phys. Lett.* **45** (1984) 1052.
16. G. K. WILLIAMSON and W. H. HALL, *Acta Metall.* **1** (1952) 22.
17. S. ENZO, M. SAMPOLI, G. COCCO, L. SCHIFFINI and L. BATTEZZATI, *Phil. Mag. B* **59** (1989) 169.
18. K. H. BUSCHOW, *J. Phys. F* **13** (1983) 563.
19. J. F. JONGSTE, M. A. HOLLANDERS, B. J. THIJSSE and E. J. MITTEMEIJE, *Mater. Sci. Engng* **97** (1988) 101.
20. M. A. HOLLANDERS and B. J. THIJSSE, *J. Non-Cryst. Solids* **117/118** (1990) 696.
21. L. NATTEZZATI, G. COCCO, L. SCHIFFINI and S. ENZO, *Mater. Sci. Engng* **97** (1988) 121.
22. R. B. SCHWARZ, R. R. PETRICH and C. K. SAW, *J. Non-Cryst. Solids* **76** (1985) 281.
23. O. KUBASCHEWSKI, *Trans. Faraday Soc.* **54** (1958) 814.
24. U. GOSELE and K. N. TU, *J. Appl. Phys.* **53** (1982) 3252.
25. M. ATZMON, K. M. UNRUH, and W. L. JOHNSON, *J. Appl. Phys.* **58** (1985) 3865.
26. M. KITADA, N. SHIMIZU and T. SHIMOTSU, *J. Mater. Sci. Lett.* **8** (1989) 1393.

Received 8 October 1991
and accepted 7 April 1992